

H II regions and IRAS PSC sources: the reliability of the association*

C. Codella¹, M. Felli², and V. Natale³

¹ Dipartimento di Astronomia e Scienza dello Spazio, Università di Firenze Largo E. Fermi 5, I-50125 Firenze, Italy

² Osservatorio Astrofisico di Arcetri, Largo E. Fermi 5, I-50125 Firenze, Italy

³ C.N.R., C.A.I.S.M.I., Largo E. Fermi 5, I-50125 Firenze, Italy

Received 24 May 1993 / Accepted 7 October 1993

Abstract. The IRAS Point Source Catalogue has been compared with a catalogue of 462 (diffuse) H II regions detected in hydrogen radio recombination lines. To distinguish the true IRAS counterpart of the H II region from chance coincidences the distribution of offset and the position in colour-colour plots as a function of $F(60 \mu\text{m})$ are investigated. It is found that sources with $F(60 \mu\text{m}) < 100 \text{ Jy}$ have a high probability of being chance coincidences. The far infrared properties of the H II regions are investigated for a subsample of 252 IRAS PSC sources which have a high ($> 80\%$) probability of being true coincidences. The majority satisfy the Wood and Churchwell colour criteria which identify ultracompact H II regions; therefore, these criteria select ultracompact as well as more diffuse H II regions, or, alternatively, diffuse H II and ultracompact H II regions may often be mixed, as predicted by the sequential star formation theory.

The luminosity of a single star required to produce the observed H II line emission correlates very well with the far infrared luminosity and is, on the average, higher than the observed value. Consequently, the stars ionizing the extended H II regions can account for the bulk of the observed FIR emission and no contribution from lower mass stars of the cluster is necessary.

Key words: H II regions – radio lines: interstellar – stars: formation – infrared: continuum: ISM

1. Introduction

Diffuse H II regions, a later phase in the evolution of a star forming region, can be investigated via observations in the far infrared. In fact, as long as they are surrounded by dust and the

Send offprint requests to: C. Codella

* Table 1 is only available in electronic form: see the editorial in A&A 1992, Vol. 266 N°2, page E1

dust optical depth is high, the stellar radiation is converted to far infrared emission (Panagia 1974; Churchwell et al. 1990b and references therein; MacLeod & Hughes 1991). Therefore the IRAS Point Source Catalogue (IRAS PSC) is an important resource tool to search for optically obscured star forming regions and it has been used extensively for this purpose (Chini et al. 1986; Beichman et al. 1986; Emerson 1987; Richards et al. 1987; Wouterloot & Walmsley 1986; Scalise et al. 1989; Palla et al. 1991; Hughes & MacLeod 1993).

Hughes & MacLeod (1989), using the IRAS emission associated with 28 H II regions selected from radio and optical catalogues (Sharpless 1959; Blitz et al. 1982), have proposed criteria to identify IRAS PSC sources associated with H II regions based on the FIR colours $[25-12]^1$, $[60-25]$ and on the $100 \mu\text{m}$ flux density.

Wood & Churchwell (1989a) have studied IRAS emission from ultracompact H II (UCH II) regions, defined as an earlier phase in the evolution of a star-forming region, when massive newly formed star(s) are still deeply embedded in the parent molecular cloud. The parameters that define an UCH II region are: size $\leq 0.1 \text{ pc}$, electron density $\geq 10^4 \text{ cm}^{-3}$ and emission measure $\geq 10^7 \text{ pc cm}^{-6}$ (Wood and Churchwell, 1989b). IRAS PSC sources associated with UCH II regions have FIR emission typically 3 to 4 orders of magnitude above the extrapolation of the radio free-free flux densities and very similar IRAS flux density distributions. From the analysis of a sample of 75 objects Wood & Churchwell (1989a) associate the IRAS PSC sources with UCH II regions, based only on the $[25-12]$ and $[60-12]$ colours.

Criteria based only on IRAS colours are not sensitive to the flux densities of the IRAS PSC source and may suffer from contamination by background sources. In this paper we examine a large list of well identified H II regions to estimate the percentage of chance associations that may contaminate samples selected by IRAS colour criteria.

¹ $[i-j] \equiv \log [F_i/F_j]$

Lockman (1989) has catalogued 462 H II regions detected in hydrogen radio recombination lines (primarily H85 α , H87 α and H88 α). His search list contained about 500 radio continuum sources chosen from galactic radio surveys (primarily the atlas of galactic radio sources of Altenhoff et al. 1978) with a peak flux density ≥ 1 Jy per beam. Given the beam used in Lockman's survey (HPBW $\simeq 3'$ at 3 cm), the list contains many diffuse H II regions, with low surface brightness but large integrated fluxes. Lockman's list is the widest database ever used to investigate the association between IRAS PSC sources and H II regions and the one which best matches the resolution of the IRAS PSC survey. In Sects. 2, 3 and 4 of this paper the criteria used to associate an IRAS PSC source with an H II region and the reliability of that association are described; in Sect. 5 the properties of the IRAS PSC sources associated with Lockman's sample are discussed; the conclusions are summarized in Sect. 6.

2. Association between H II regions and IRAS PSC sources

In the Lockman sample 17 sources have identical coordinates to another source, but are listed as two different entries, because the recombination line spectrum has two well separated velocity peaks (difference ≥ 27 km s $^{-1}$). Therefore for the cross-correlation with the positions in the IRAS PSC we have used a list of 445 H II regions; each "double-line" position will be considered as a single source.

In order to associate an IRAS PSC source with an H II region we used the following criteria:

1. coincidence within a radius of 120'' around the H II region position; this value allows for the beam width of the antenna used by Lockman and IRAS positional error. The second depends on the nature of the IRAS PSC sources, but is usually better than 20'' (Beichman et al. 1985).
2. IRAS PSC sources known to be associated with extragalactic sources have been excluded (Beichman et al. 1985).

For 288 H II regions (65% of the whole sample) we find a possible association with one or more IRAS PSC sources. The number of H II regions which do not have an IRAS PSC counterpart is rather large, 157. However, 18 of these are located in regions not observed by the satellite. For the remaining 139 H II regions we cannot be sure that the lack of an IRAS PSC counterpart necessarily implies a lack of FIR emission. In fact, some H II regions may be located in confused regions of the IRAS survey. For instance, Orion is not included in the Point Source Catalogue. If all the 139 H II regions do not emit at FIR wavelengths, this implies that about a third of the sources in the Lockman sample are so diffuse that the dust optical depth is negligible. It is worth noting that the subsample of H II regions not associated with IRAS PSC sources does not differ from those associated as far as the distribution of brightness temperature and width of the recombination line are concerned.

The positional coincidence is a necessary, but not sufficient condition to select infrared sources physically associated with H II regions. Unrelated background IRAS PSC sources can contaminate the associations. In order to verify the reliability of the

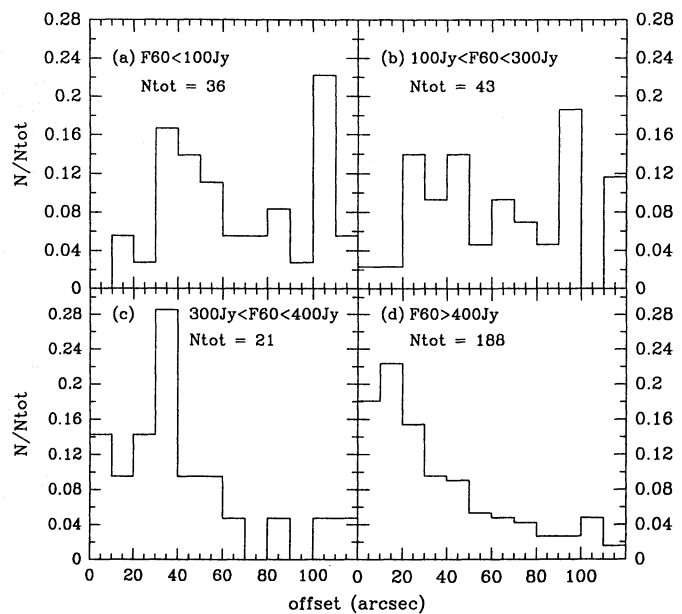


Fig. 1a–d. Offset distribution of the IRAS-H II region associations; **a** $F_{60} \leq 100$ Jy; **b** $100 \text{ Jy} < F_{60} \leq 300$ Jy; **c** $300 \text{ Jy} < F_{60} \leq 400$ Jy; **d** $F_{60} > 400$ Jy

associations two different tests were used: (i) the distribution of the offset; (ii) the position of IRAS PSC sources in colour-colour plots.

2.1. Offset distribution

The offset distribution should peak at low angular separations for true associations, while for chance associations a linear growth as a function of angular separation is expected. In order to investigate a possible dependence on the IRAS flux density, the sources have been divided into several subsamples according to the 60 μm flux density. The 60 μm band was chosen for two reasons: (i) IRAS PSC sources associated with H II regions have flux density values at 60 and 100 μm higher than those at 12 and 25 μm ; (ii) the sensitivity at 60 μm (0.5 Jy) is better than at 100 μm (1.5 Jy; Beichman et al. 1985).

The offset distribution for $F_{60} < 100$ Jy, shown in Fig. 1a (where N_{tot} stands for the number of sources of the subsample), does not show a peak at low offsets. A gradual change from this distribution to that expected for true associations is indicated in Fig. 1b, 1c and 1d, where the distributions with F_{60} between 100–300 Jy (Fig. 1b), 300–400 Jy (Fig. 1c) and greater than 400 Jy (Fig. 1d) are plotted.

Chance associations may become dominant for sources with low F_{60} , while only a negligible part of IRAS PSC sources with $F_{60} \geq 300$ Jy should be chance coincidences.

In the following, the list of H II regions associated with IRAS PSC sources has been divided into two subsamples according to F_{60} using 300 Jy as discriminator between the two classes. Class A ($F_{60} > 300$ Jy) contains 209 sources; Class B ($F_{60} \leq 300$ Jy) contains 79 sources.

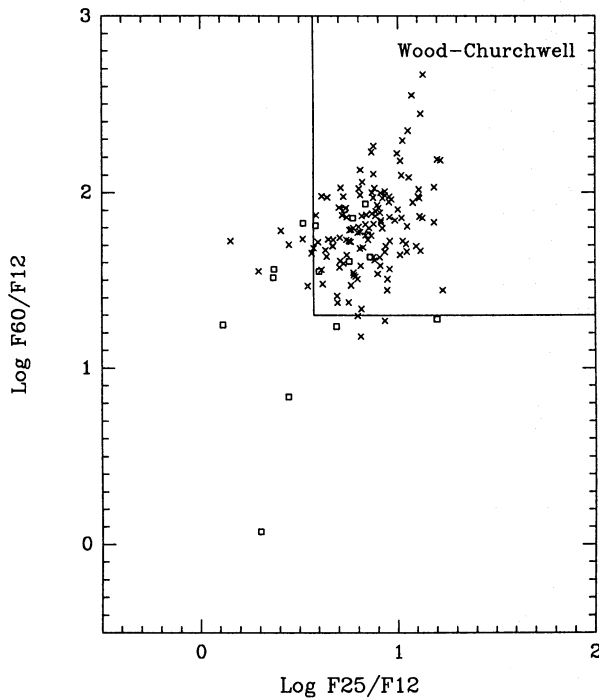


Fig. 2. [25-12]-[60-12] colour plot: distribution of the IRAS PSC sources associated with the Lockman list; crosses represent class A sources ($F_{60} > 300$ Jy), while squares represent class B sources ($F_{60} \leq 300$ Jy)

2.2. Colour-colour plots

The Hughes & MacLeod (1989) criteria to select IRAS PSC sources associated with H II regions, with a confidence level of 89% are: (i) $[25-12] \geq 0.4$; (ii) $[60-25] \geq 0.25$; $F_{100} \geq 80$ Jy. There are 112 sources without flux density upper limits in subsample A: 110 of these (98%) satisfy the HM criteria, confirming their validity. For subsample B there are 8 sources without upper limits, 7 of these satisfy the HM criteria.

The Wood & Churchwell (1989a) criteria to identify UCH II regions are: (i) $[25-12] \geq 0.57$; (ii) $[60-12] \geq 1.30$. The number of sources detected at the IRAS bands used in the WC criteria (12, 25 e 60 μm) are 132 for subsample A, 124 of which (94%) fall inside the WC box. For subsample B there are 17 sources detected, only 6 of these satisfy the WC criteria. The distribution of the two classes in the WC colour-colour plane is shown in Fig. 2.

In summary, IRAS PSC sources of subsamples A and B have different distributions in the colour-colour plots. While the bulk of subsample A falls within the WC box, the subsample B contains many sources that do not satisfy the WC criteria, these may be chance coincidences.

3. The comparison random sample

In order to estimate the expected percentage of chance associations we have produced a new list of positions by adding to the 445 Lockman sources a random offset between $\pm [3' - 10']$ both

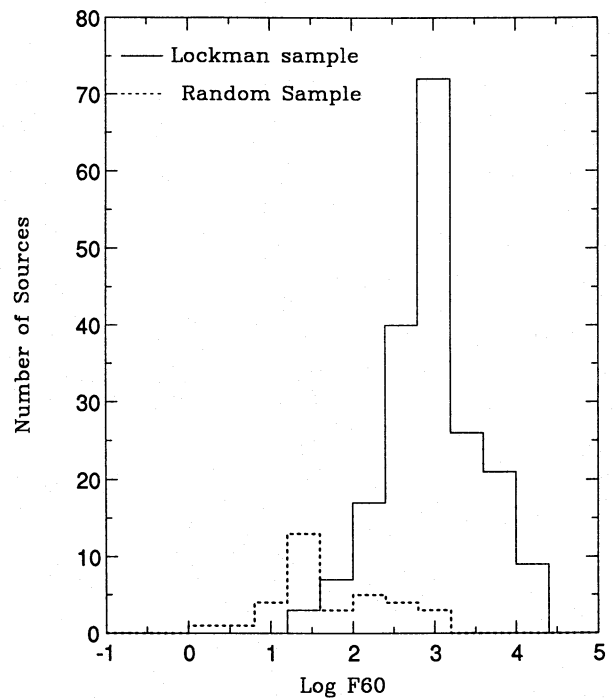


Fig. 3. 60 μm flux density distributions of the IRAS PSC sources associated with the Lockman sample and of those one associated with a random sample

to the right ascension and the declination. The new list has then been cross-correlated with the IRAS Point Source Catalogue with the same criteria previously used. For 100 positions we find an association with one or more IRAS PSC sources. Additional tests indicate that this number has an r.m.s. deviation of about 5%.

3.1. 60 μm flux density distribution

Contrary to the Lockman sample, the random sample contains a large fraction (89%) of sources with $F_{60} < 300$ Jy. Figure 3 shows the F_{60} distributions for the random and the Lockman samples (we have excluded in both samples sources with an upper limit). The two distributions are markedly different: the Lockman sample peaks at 1000 Jy, while the random sample peaks at 25 Jy. This comparison indicates that the contamination by chance associations is important only for IRAS PSC sources with low F_{60} .

3.2. Colour-colour plots

There are very few sources without upper limits in the random sample (less than 10 sources for both subsamples A and B). Therefore, it is not possible to make a direct comparison with Fig. 2.

In Fig. 4 the distribution of all the 100 IRAS PSC sources associated with the random list (including upper limits) is plotted. Note that the distributions plotted in Figs. 2 and 4 are quite

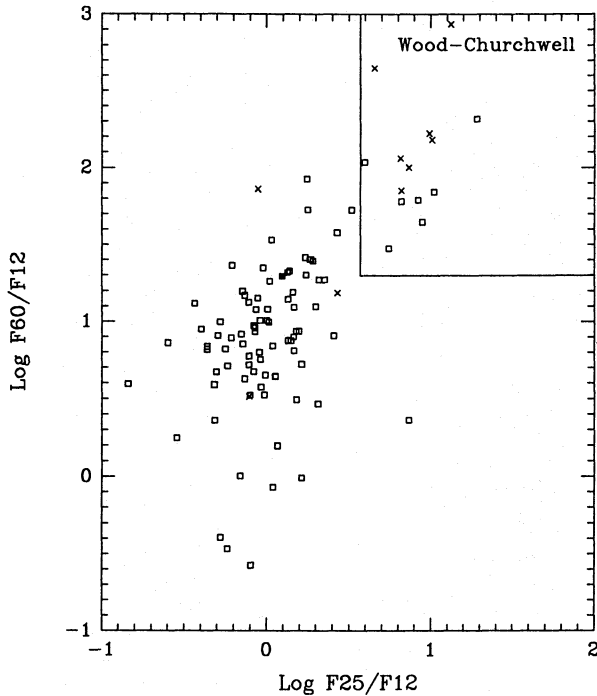


Fig. 4. [25-12]-[60-12] colour plot: distribution of the IRAS PSC sources associated with the random list; crosses represent sources with $F_{60} > 300$ Jy, while squares represent sources with $F_{60} \leq 300$ Jy

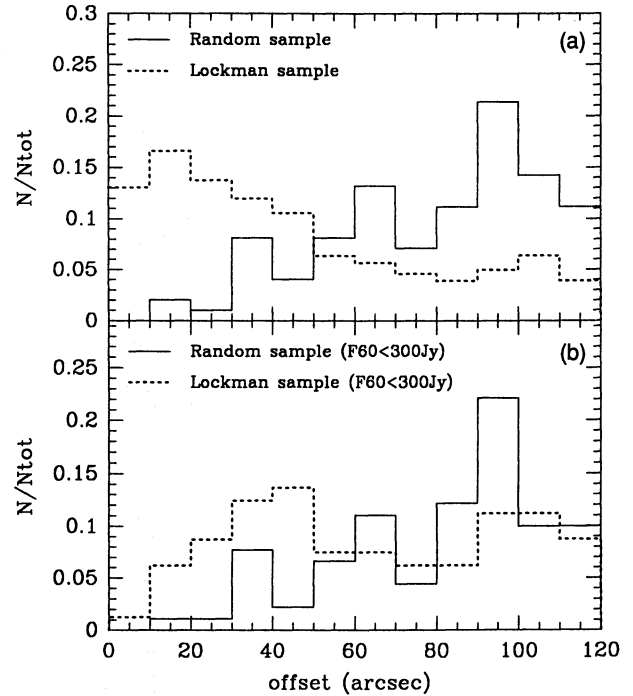


Fig. 5a and b. Comparison between the offset distributions of the IRAS PSC sources associated with the Lockman list and of those associated with a random list; (a) all sources; (b) $F_{60} \leq 300$ Jy

different: the bulk of the random IRAS PSC sources are located outside the region delimited by the WC criteria.

3.3. Offset distribution

The offset distribution in the random sample increases as a function of angular separation, as expected. We have compared the random distribution with that of Lockman's sample (Fig. 5a) and with that of subsample B (Fig. 5b); while the first two have opposite trends, subsample B has a distribution similar to the random sample. Therefore, the majority of the IRAS PSC sources of subsample B may be chance associations.

4. Reliability of the IRAS PSC source-H II region associations

In order to estimate the reliability of an association as a function of offset and F_{60} , we need to know the number, N_r , of chance associations contained among the Lockman sample.

N_r should be lower than the number of IRAS PSC sources associated with the random positions, because Lockman's H II regions with a true IRAS PSC association have a negligible probability of having a random association. N_r can be estimated, reducing the number of the IRAS PSC sources associated with the random list by a factor $[1-(T/N)]$ (White et al. 1991), where N is the total number in the Lockman list (445) and T is the number of H II regions with a true IRAS PSC association. An estimate of T can be derived from the difference between the numbers of the

IRAS PSC sources associated with the two samples (including multiple associations); N_r is then equal to 53.

Under the assumption that the population of chance associations in the Lockman sample has the same properties as the random sample, Fig. 6 compares the offset distribution of the Lockman list (continuous line) and that of the subsample containing the estimated 53 chance associations (dotted line). The dashed line represents the probability that an association is a true counterpart. The reliability of an association decreases for larger values of the offset. For offsets less than $80''$, the probability of a true association is greater than 50%.

Figure 7 compares the F_{60} distributions for the two samples. The reliability is very high (>80%) for sources with $F_{60} > 100$ Jy and decreases rapidly towards lower fluxes. The triangles indicate the function that fits the reliability distribution:

$$P(x) = 50 [1 + \tanh(2x + 3)] \quad (1)$$

where: $x \equiv \text{Log } F_{60}$.

White et al. (1991) have investigated the properties of the IRAS PSC sources associated with 1992 compact VLA radio (20 cm) sources from an unbiased survey of a strip of the galactic plane (Zoonematkerani et al. 1990). They have selected 294 IRAS PSC sources with high probability (>50%) of being true associations, 198 of which are classified (using the WC colours criteria) as UCH II regions or candidate UCH II regions. All their UCH II regions have $F_{60} > 100$ Jy, in very good agreement with the present results.

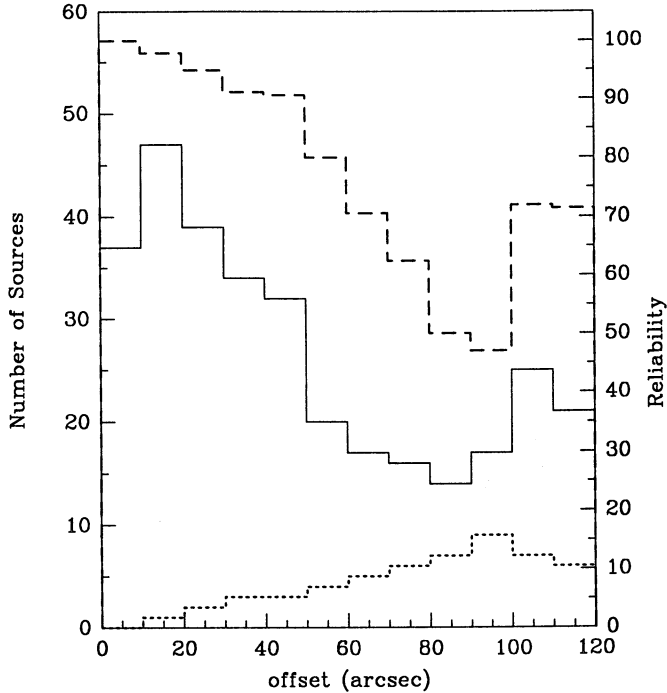


Fig. 6. Comparison between the offset distribution of the IRAS PSC sources associated with the Lockman list (continuous line) and of the subsample that contains chance associations (dotted line). The dashed line represents the probability of an IRAS PSC source being a true counterpart

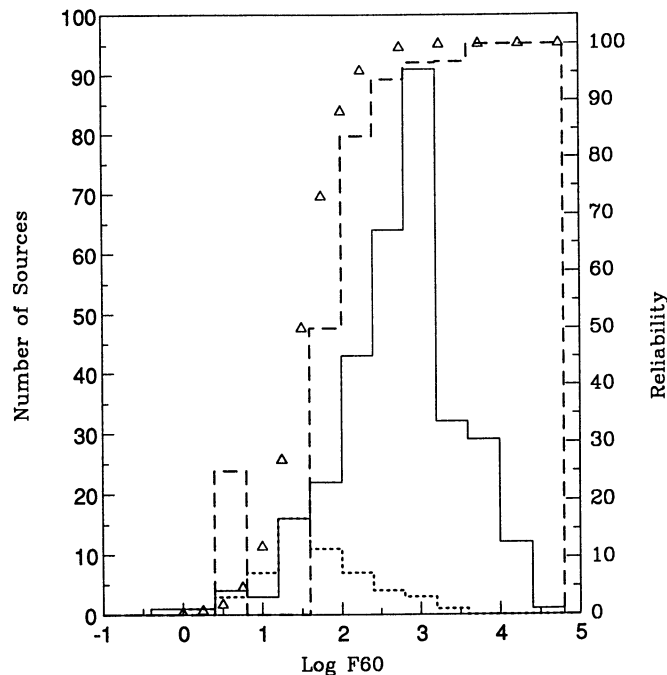


Fig. 7. Comparison between the F_{60} distribution of the Lockman (continuous line) and random list (dotted line). The dashed line represents the probability of an IRAS PSC source being a true counterpart. The triangles indicate the function that fits the reliability distribution

5. Properties of IRAS PSC sources associated with H II regions

The previous conclusions show that IRAS PSC sources with $F_{60} > 100$ Jy (252 sources) have a probability $>80\%$ of being associated with H II regions. In this section, we investigate their infrared properties. Table 1 lists: equatorial (1950) and galactic coordinates, distance and height from the galactic plane (see Sect. 5.2), name of the associated IRAS PSC source, the four IRAS flux densities, the integrated infrared flux (computed following Henning et al. 1990) and the IRAS luminosity L_{FIR} . The last column is for comments: 'D' indicates positions that contain two H II regions at a different v_{lsr} ; 'UCHII' stands for IRAS PSC sources that satisfy the WC colour criteria; finally, 'O' identifies H II regions with an UC radio component observed either at 2, 6 or 20 cm.

5.1. Diffuse and UCH II regions

Lockman's list should be more representative of diffuse H II regions, because the large beam is sensitive to faint extended emission, which can give a contribution to the total continuum and line flux densities larger than that of UCH II regions. It is interesting to see if the colour-colour criteria can discriminate between the two evolutionary phases. 145 out of the 252 IRAS PSC-H II region associations satisfy the WC colour criteria (including also the sources with upper limit at $12 \mu\text{m}$, because this upper limit cannot shift the IRAS PSC sources away from the WC region). If we exclude the sources with upper limits at 12, 25 and $60 \mu\text{m}$, then 94% satisfy the WC criteria. Therefore, the WC colour criteria select not only UCH II regions, but also diffuse regions, or, alternatively, diffuse H II and UCH II regions may often be mixed.

Wood & Churchwell (1989a) have selected from the IRAS Point Source Catalogue 1646 UCH II candidates in the Galaxy; their aim was to estimate the total number of newly formed massive stars still embedded in molecular clouds. From the number found they concluded that the age of an UCH II region could be a substantial fraction ($\approx 10\%$) of the star's lifetime. Since the present results indicate that the Wood and Churchwell sample may: (i) contain also diffuse H II regions, (ii) suffer from a contamination of background sources with low density fluxes, the UCH II population and lifetime may have been overestimated.

Lockman's list has been cross-correlated with catalogues of UCH II regions (Wood & Churchwell 1989b; Churchwell 1990 and references therein; Churchwell et al. 1990a and references therein; White et al. 1991; Kurtz et al. 1993). 135 H II regions (out of 445 objects) are associated with UCH IIs; 114 of these have an IRAS PSC counterpart, 88 with the colour of UCH II regions. Although the two lists are heterogeneous, the large number found suggests that diffuse and UCH II regions co-exist quite often and that the sequential star formation processes (Elmegreen & Lada 1977; Habing & Israel 1979 and references therein; Shu et al. 1987 and references therein) is operative in about a third of the star forming regions.

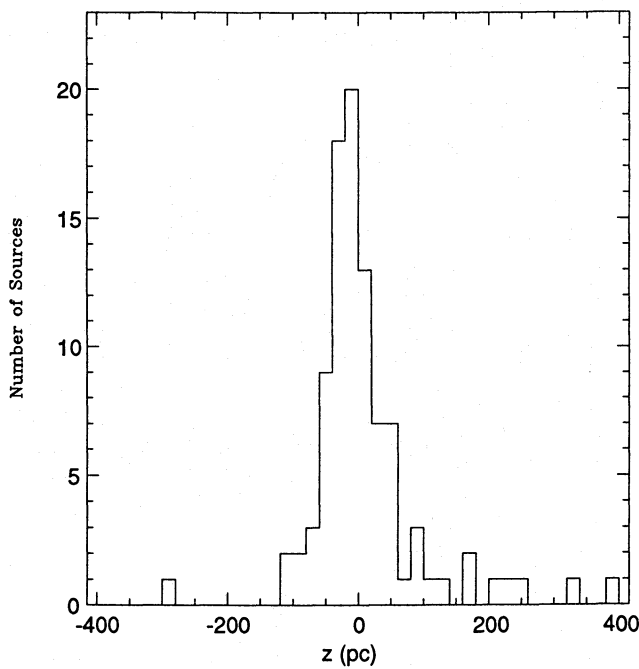


Fig. 8. H II regions z distribution

5.2. Distances and galactic distribution

The kinematic distances have been obtained from hydrogen recombination line velocities using the rotation curve of Brand (1986), which has an orbital velocity of 220 km s^{-1} at the Sun orbital radius (8.5 kpc). For the calculation of distances, we have excluded positions with two recombination lines.

To resolve the near/far distance ambiguity within the solar circle, distances were compared with those given in other catalogues, primarily Solomon et al. (1987). The authors have observed CO emission toward a sample of giant molecular clouds and have used several techniques to resolve the distance ambiguity. For some sources the catalogue of Wink et al. (1982) was used, which is based on the observations of two hydrogen recombination lines (H76 α and H90 α).

Sources with an uncertainty greater than a factor of 1.5 were rejected; consequently all distances that do not satisfy the following relationships: $(\Delta d)_1/d < 0.50$ e $(\Delta d)_2/d > -0.33$ were excluded, where $(\Delta d)_1$ and $(\Delta d)_2$ represent the uncertainties produced by changing the velocity by $\pm 5 \text{ km s}^{-1}$. Finally, the distance of sources with height from the galactic plane greater than 800 pc were rejected. After this, distances of 95 H II regions were obtained. Figure 8 shows a histogram of the distribution of height from the galactic plane: the FWHM is 78 pc. This is larger than that of O-stars in the Galaxy (50 pc; Mihalas & Binney 1981); consequently our sample may contain B-type stars, which have a larger scale height than O-stars.

For the 95 sources with known distance, the IRAS luminosity (L_{FIR}) has been calculated. Figure 9 shows the L_{FIR} distribution, which peaks at $3 \cdot 10^5 L_{\odot}$.

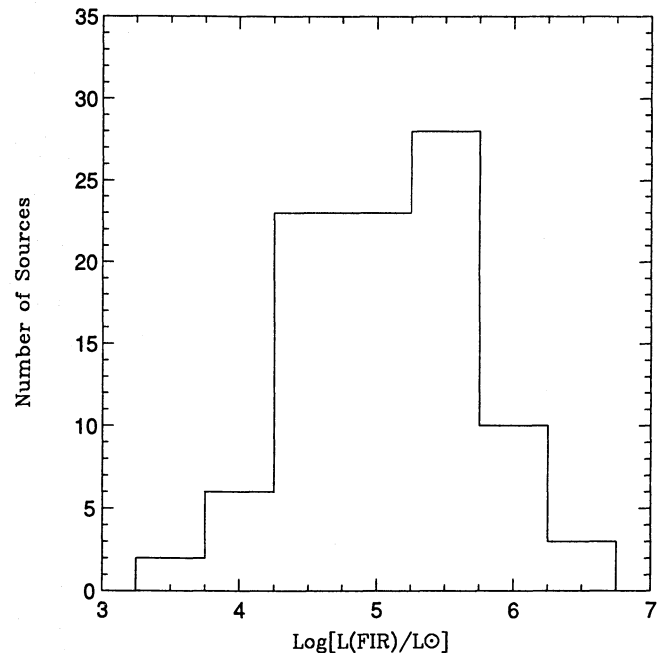


Fig. 9. IRAS luminosity distribution of the sources with known distance

5.3. Flux and luminosity correlations

In Fig. 10 the IRAS integrated flux (for sources without upper limits) is plotted against the parameter $w = 1.0645 T_l \Delta v$ (mK km s^{-1}), where T_l and Δv are respectively the temperature and the FWHM of the observed recombination line (Lockman 1989).

Assuming a gaussian profile the parameter w is proportional to the intensity of the observed line. w and F_{FIR} are well correlated. The linear fit gives:

$$\text{Log } F_{FIR} (\text{watt m}^{-2}) = 0.93 \text{ Log } w (\text{mK km s}^{-1}) - 12.87(2)$$

The integrated infrared emission should approximate the bolometric luminosity of the star(s) inside the H II region, if we assume that all the stellar flux is converted to far infrared emission by dust. At the same time, the intensities of the observed hydrogen recombination lines give an estimate of the stellar ionizing flux emitted by the most luminous, massive stars.

It is interesting to compare L_{FIR} with the luminosity (L_{RAD}) of a single star that would be required to produce the observed line intensity. We calculated the excitation parameter U (cm pc^{-2}) from the parameter w (for sources with known distance) and the luminosity L_{RAD} using Panagia's (1973) conversion table. In Fig. 11 L_{RAD} is plotted against L_{FIR} .

The error associated with L_{FIR} includes uncertainties in distance and the four IRAS flux densities, while the error associated with L_{RAD} includes: (i) distance; (ii) width and line temperature of the hydrogen line; (iii) deviation of the electron temperature from an assumed 10^4 K .

Figure 11 shows that L_{RAD} correlates very well with L_{FIR} ; this indicates that our results are consistent with Panagia's

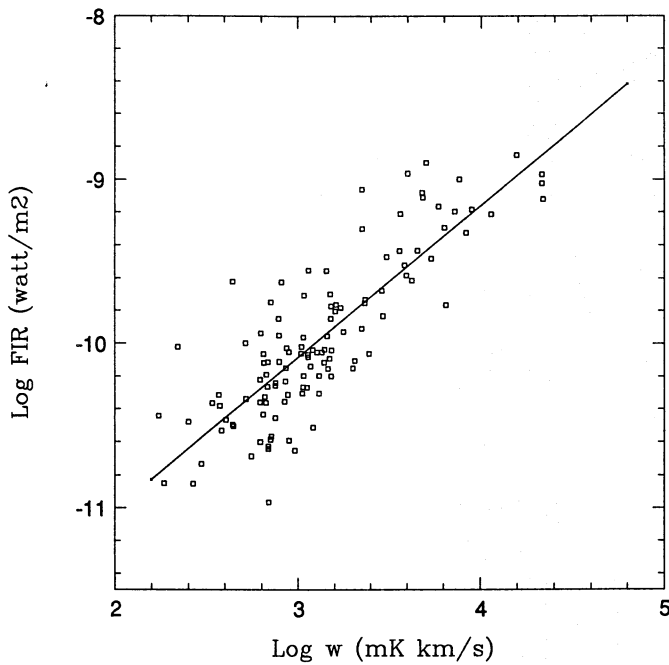


Fig. 10. IRAS integrated flux vs. integrated flux intensity w . The continuous line represents the best linear fit

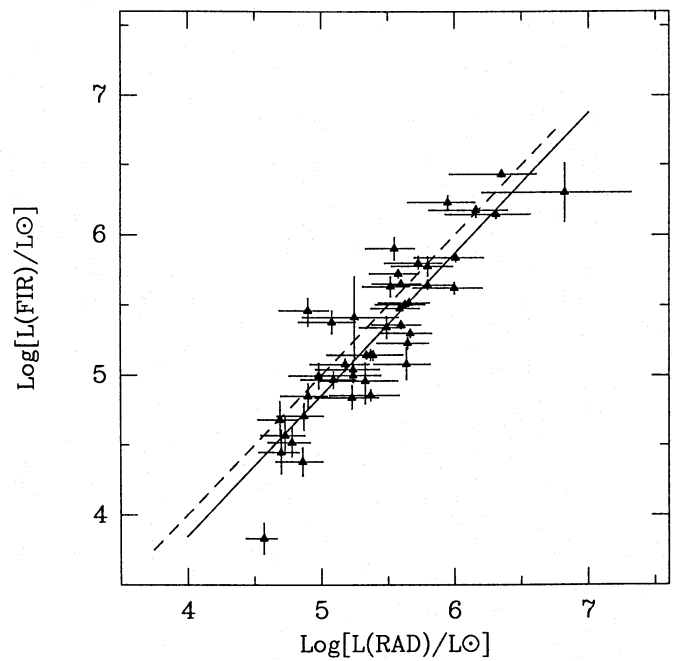


Fig. 11. Plot of L_{RAD} vs. L_{FIR} . The dashed line represents $L_{RAD}=L_{FIR}$. The continuous line represents the best linear fit

model. The continuous line in Fig. 11 represents the best linear fit:

$$\text{Log } L_{FIR} (L_{\odot}) = 1.01 \text{ Log } L_{RAD} (L_{\odot}) - 0.19 \quad (3)$$

This relation indicates a ratio $L_{FIR}/L_{RAD} \simeq 0.65$ and suggests that dust grains convert almost but not all the stellar flux to infrared emission. For our sample of (diffuse) H II regions, the contribution to IRAS emission from non-ionizing later spectral type stars is not necessary. Kurtz et al. (1993) have analysed the infrared properties of a sample of UCH II region; they have concluded that the combined infrared luminosities of all non-ionizing stars associated with UCH II regions is required and is not negligible relative to that of the more massive stars. This discrepancy may depend on the type of H II region considered. If the H II region is deeply embedded in a molecular cloud (as are UCH II regions, with large dust optical depth), then dust converts almost all the stellar emission to FIR radiation, but if the H II region is diffuse and has a low dust optical depth, dust may intercept only a small fraction of the stellar radiation.

The correlation between L_{RAD} and L_{FIR} is also an independent check of the reliability of the association between H II regions and IRAS sources.

6. Conclusions

The IRAS properties of a sample of 445 H II regions is investigated. 288 (65%) sources are associated with IRAS PSC sources. In order to determine the probability of an IRAS PSC source being a true counterpart we have examined a random sample; the analysis shows that: (i) the offset distribution grows

linearly as a function of the angular separation; (ii) the $60 \mu\text{m}$ flux density distribution peaks at about 25 Jy. The number of chance associations among our sample was estimated and used to calculate the probability, as a function of offset and of F_{60} , that an IRAS PSC source is a true association. The probability of association increases for lower values of offset; sources with offset smaller than $80''$ have a probability greater than 50% of being a true counterpart. Moreover the reliability is very high (>80%) for sources with $F_{60} > 100$ Jy and rapidly decreases for sources with lower flux density.

In order to analyse infrared properties of H II regions, 252 sources with $F_{60} > 100$ Jy were selected. The confidence of the criteria of Hughes & MacLeod (1989) to identify H II regions is confirmed. The sample also satisfies the colour criteria of Wood & Churchwell (1989a) that identify UCH II regions. Therefore, these criteria select not only UCH II regions, but also diffuse regions. The cross-correlation between Lockman's diffuse H II regions and catalogues of UCH II regions confirms that the two classes overlap quite often, as predicted by the sequential star formation theory.

The intensity of the hydrogen recombination line and of the IRAS emission are well correlated. The total luminosity (L_{RAD}) of a single star that would be required to ionize the H II regions correlates very well with L_{FIR} ; therefore the stars producing the extended H II regions are responsible for the bulk of the observed IRAS emission. Consequently, for our sample of (diffuse) H II regions, the contribution to IRAS emission from non-ionizing low mass stars is not required to explain the relationship between L_{RAD} and L_{FIR} .

References

- Altenhoff, W.J., Downes, D., Pauls, T., Schraml, J., 1978, *A&AS*, 35, 23
- Beichman, C.A., Neugebauer, G., Habing, H.J., Clegg, P.E., Chester, T.J., 1985, *IRAS Catalogs and Atlases*, Washington
- Beichman, C.A., Myers, P.C., Emerson, et al., 1986, *ApJ*, 307, 337
- Blitz, L., Fich, M., Stark, A.A., 1982, *ApJS*, 49, 183
- Brand, J., 1986, Ph.D. Thesis, Leiden University
- Chini, R., Kreysa, E., Mezger, P.G., Gemund, H.R., 1986, *A&A*, 154, L8
- Churchwell, E., 1990, *A&AR*, 2, 79
- Churchwell, E., Walmsley, C.M., Cesaroni, R., 1990a, *A&AS*, 83, 119
- Churchwell, E., Wolfire, M.G., Wood, D.O.S., 1990b, *ApJ*, 354, 247
- Elmegreen, B.G., Lada, C.J., 1977, *ApJ*, 214, 725
- Emerson, J.P., 1987, *Star Forming Regions*, Dordrecht Reidel: Peimbert and Jugaku eds.
- Habing, H.J., Israel, F.P., *A&AR*, 17, 345
- Henning, T.H., Pfau, W., Altenhoff, W.J., 1990, *A&A*, 227, 542
- Hughes, V.A., MacLeod, G.C., 1989, *A&A*, 97, 786
- Hughes, V.A., MacLeod, G.C., 1993, *AJ*, in press
- Kurtz, S., Churchwell, E., Wood, D.O.S., 1993, *ApJS*, in press
- Lockman, F.J., 1989, *ApJS*, 71, 469
- MacLeod, G.C., Hughes, V.A., 1991, *AJ*, 102, 658
- Mihalas, D., Binney, J., 1981, *Galactic Astronomy*, 2d ed., San Francisco: Freeman ed.
- Palla, F., Brand, J., Cesaroni, R., Comoretto, G., Felli, M., 1991, *A&A*, 246, 249
- Panagia, N., 1973, *AJ*, 78, 929
- Panagia, N., 1974, *ApJ*, 192, 221
- Richards, P.J., Little, L.T., Toriseva, M., Heaton, B.D., 1987, *MNRAS*, 228, 43
- Scalise, E.Jr, Rodriguez, L.F., Mendoza-Torres, E., 1989, *A&A*, 221, 105
- Schraml, J., Mezger, P.G., 1969, *ApJ*, 156, 269
- Sharpless, S., 1959, *ApJS*, 4, 257
- Shu, F.H., Adams, F.C., Lizano, S., 1987, *A&AR*, 25, 23
- Solomon, P.M., Rivolo, A.R., Barrett, J., Yahil, A., 1987, *ApJ*, 319, 730
- White, R.L., Becker, R.H., Helfand, D.J., 1991, *ApJ*, 371, 148
- Wink, J.E., Altenhoff, W.J., Mezger, P.G., 1982, *A&A*, 108, 227
- Wood, D.O.S., Churchwell, E., 1989a, *ApJ*, 340, 265
- Wood, D.O.S., Churchwell, E., 1989b, *ApJS*, 69, 831
- Wouterloot, J.G.A., Walmsley, C.M., 1986, *A&A*, 168, 237
- Zoonematkerani, S., Helfand, D.J., Becker, R.H., White, R.L., Perley, R.A., 1990, *ApJS*, 74, 181